



# INVESTIGATE THE INHIBITION AGAINST BACTERIA BY USING SCHIFF BASE COMPLEXES

A. Alshamiry, J.M.S. Alshawi\*

Chemistry Department, College of Education for Pure Sciences, Basrah University, Basrah, Iraq.

[jasim.salih@uobasrah.edu.iq](mailto:jasim.salih@uobasrah.edu.iq)

Article history:	Abstract:
<b>Received:</b> 7 <sup>th</sup> May 2024 <b>Accepted:</b> 4 <sup>th</sup> June 2024	FT-IR, UV-vis, <sup>1</sup> H-NMR, <sup>13</sup> C, and mass spectrometry were used to characterize the ligand, and complexes it was discovered that the synthesized ligand was donation as (NO) <sup>1</sup> . The produced ligand reacted with a few transition elements, such as Cu <sup>2+</sup> , Co <sup>2+</sup> , and Ni <sup>2+</sup> , to form complexes, which were then characterized by conductivity, FT-IR, UV-vis, and spectroscopy. Low values for (IR), mass spectrum, and molar conductivity suggest that the complexes lack negative radicals outside of the coordination sphere. The complexes were also evaluated for their magnetic properties using thermogravimetric analysis (TGA), which revealed that the cobalt (II), copper (II), and nickel (II) complexes have paramagnetic properties and adopt an octahedral geometry. TGA was also used to determine whether the complexes contain water molecules coordinated to the central atom. The complexes' structural formulae were suggested using the various characterization techniques. The compounds under investigation proved efficient against both positive and negative bacteria, allowing us to move forward with theoretical and biological research to determine the precise location where bacteria's protein's function.

**Keywords:** Schiff base; Transition metals; Biological.

## 1. INTRODUCTION

Shortly protein's discovery, Schiff bases were extremely important for a variety of reasons, one of which being that they could be used as building blocks to produce heterocyclic compounds and their metal complexes. Additionally, they have been utilized in the synthesis of several polymers with the ability to withstand oxidation, heat, light, and superconductivity. There are Schiff base derivatives that are biologically active and contribute significantly to bioactivity, such as in enzymatic transport reactions. Additionally, certain Schiff base types are combined with liquid polymers to enhance their specific characteristics. Pigments for printing and ink are made using specific Schiff base types (Du et al., 2007; Lidskog et al., 2020; Maleev et al., 2014).

Since their creation, Schiff bases have been employed in a wide range of real-world situations and are preferred for their adaptability in complex formation. These complexes' transition elements could be used as models for species that are significant to biology.

Aggressive cells are a feature of a class of disorders known as cancer or malignant tumors. A malignant tumor is characterized by its proliferating cells, which have the capacity to penetrate and destroy nearby tissues. Most people fear getting a diagnosis because the illness is still a major global public health concern. In industrialized and developing nations, it is the second most common cause of death after cardiovascular disease. In these same countries, cancer ranks second in terms of mortality. Surgery, chemotherapy, and radiation therapy are currently the mainstays of cancer treatment; but, recent advancements in research have made it possible to develop medications that target cancer cells by distinguishing them at the molecular level (Al-Zaidi et al., 2019; Garba et al., 2021).

The pharmacological properties of complexes that arise from the interaction of certain transition metals with Schiff bases include antitumor and antithyroid properties, as well as application in the treatment of bacterial infections (Ashoor et al., 2020; Bejaoui et al., 2019; Taylor et al., 2014).

This study examined the biological effectiveness of Schiff base and the complexes made from it with both positive and negative microorganisms.

## 2. EXPERIMENTAL

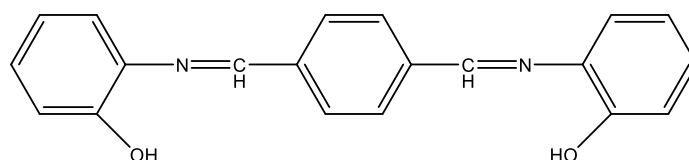
### 2.1 Materials and Methods

Merck supplied all of the reagents that were utilized. KBr pellets were utilized to record infrared spectra in the 400–4000  $\text{cm}^{-1}$  range using a Shimadzu FTIR spectrometer, model number 8400 S. A Thermo Fisher device was used to calculate melting points. The  $^1\text{H}$ NMR spectrum of DMSO was recorded using a Bruker 400 MHz NMR spectrometer. The conductivity in DMF at room temperature is measured with a Jenway PCMB conductivity meter. The UV-visible spectrum was recorded in DMF using a German SPV-725 spectrometer. Based on the Gouy method, the magnetic characteristics were measured at room temperature using  $\text{Hg}[\text{Co}(\text{NCS})_4]$  as a standard.

### 2.2 Synthesis of the ligand and its metal complexes

The ligand's general synthesis pathway, (L). In a flask with a round bottom, 2 mmol (0.218 gm) of 2-amino phenol was dissolved in 20 ml of 100% ethanol to create L1. When the mixture reached boiling point, two drops of glacial acetic acid were added as a catalyst, and the mixture was then agitated for 30 minutes while dropping 1 mmol (0.134gm) of terephthalaldehyde diluted in 20 ml of pure ethanol. Reflux was used to heat the reaction mixture for three hours while stirring continuously. TLC was used to observe the reaction. Orange precipitate appeared when the reaction mixture was refrigerated until the following day. After removing the orange precipitate, ethanol was used to recrystallize it. Equation (2.1) indicates an 83% reaction yield (Fadhil et al., 2024; Savalia et al., 2013). **Scheme 1.**

Orange color; yield: 77 %; M.P 224-225 °C; **FTIR** ( $\nu\text{cm}^{-1}$ ): 3365 ( $\nu\text{OH}$ ), 3026 ( $\nu\text{CH}$  aromatic), 1632 ( $\nu\text{C}=\text{N}$ ), 1242 ( $\nu\text{C}=\text{O}$ ), 1587 ( $\nu\text{C}=\text{C}$ );  **$^1\text{H}$  NMR** (DMSO, 400 MHz;  $\delta$  ppm)  $\delta$ : 11.1(s, 1H, OH), 8.8 (s, 2H, 2CH =N), 8.1-6.68 (m, 10H, Ar-H);  **$^{13}\text{C}$  NMR** (DMSO, 100 MHz;  $\delta$  ppm): 116-139 (aromatic carbons), 151(-C-O); 158 (CH=N); **MS: m/z:** 316[M+]; UV-vis. in DMSO,  $\text{cm}^{-1}$  (transition): 285 ( $n\rightarrow\pi^*$ ) and 435 ( $n\rightarrow\pi^*$ ) (Annapure et al., 2016; Vishwa et al., 2024).



**Scheme 1**

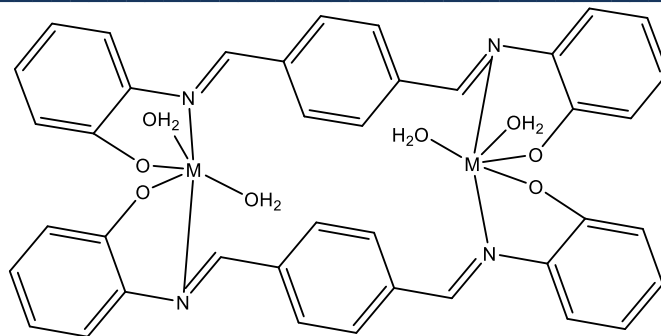
### 2.3 Synthesis of metal complexes

According to the chemistry literature, a number of complexes were created by reacting the produced Schiff bases with metals.

One millimole (0.170 gm) of copper(II) ion as chloride and One millimole (0.316 gm) of ligand L dissolved in twenty milliliters of 99% ethanol were combined to create the LCu complex. 0.170 gm of Cu(II) ion as chloride, which was added in stages to a 100 ml round-bottom flask by flash distillation and heated for 4 hours after dissolving in 20 ml of 99% ethanol. After that, the precipitate was collected, dried, and colored dark brown (63% yield). It was then sterilized with ether.

The preparation of the LNi, LCo complexes were carried out by mixing 1mmol (0.316gm) of ligand L with 1mmol (0.2379gm) of Nickel(II) and (0.2377gm) Cobalt(II) ion, respectively (Kalaivani et al., 2012; Taha et al., 2022). **Scheme 2.**

**Complex LCo.** Brown color; yield: 61 %; M. P>300 °C; FTIR ( $\nu\text{cm}^{-1}$ ): 1622 ( $\nu\text{C}=\text{N}$ ), 1589 ( $\nu\text{C}=\text{C}$ ), 3174 ( $\nu\text{CH}$  aromatic), 563 ( $\nu\text{M}-\text{N}$ ) and 501 ( $\nu\text{M}-\text{O}$ ); **UV-vis**, in DMF,  $\text{cm}^{-1}$  (transition): 285 ( $n\rightarrow\pi^*$ ), 385 ( $n\rightarrow\pi^*$ ) and 540 (d-d); MS: m/z: 318[M+]. **Complex LCu,** Pale brown color; yield: 65 %; M. P>300 °C; FTIR ( $\nu\text{cm}^{-1}$ ): 1693 ( $\nu\text{C}=\text{N}$ ), 1580 ( $\nu\text{C}=\text{C}$ ), 3020 ( $\nu\text{CH}$  aromatic), 582 ( $\nu\text{M}-\text{N}$ ) and 490 ( $\nu\text{M}-\text{O}$ ); **UV-vis**, in DMF,  $\text{cm}^{-1}$  (transition): 290 ( $n\rightarrow\pi^*$ ), 380 ( $n\rightarrow\pi^*$ ), 560, 620 (d-d), MS: m/z: 326[M+H]<sup>+</sup>. **Complex LNi.** Dark brown color; yield: 60%; M. P>300 °C; FTIR ( $\nu\text{cm}^{-1}$ ): 1622 ( $\nu\text{C}=\text{N}$ ), 1589 ( $\nu\text{C}=\text{C}$ ), 3050 ( $\nu\text{CH}$  aromatic), 540 ( $\nu\text{M}-\text{N}$ ) and 500 ( $\nu\text{M}-\text{O}$ ); **UV-vis**, in DMF,  $\text{cm}^{-1}$  (transition): 290 ( $n\rightarrow\pi^*$ ), 385 ( $n\rightarrow\pi^*$ ) and 520, 580 (d-d); MS: m/z: 316[M+4H]<sup>+</sup> (Alshawi et al., 2020; Reddy et al., 2016).



Scheme 2. M= Cu<sup>2+</sup>, Co<sup>2+</sup>, Ni<sup>2+</sup>

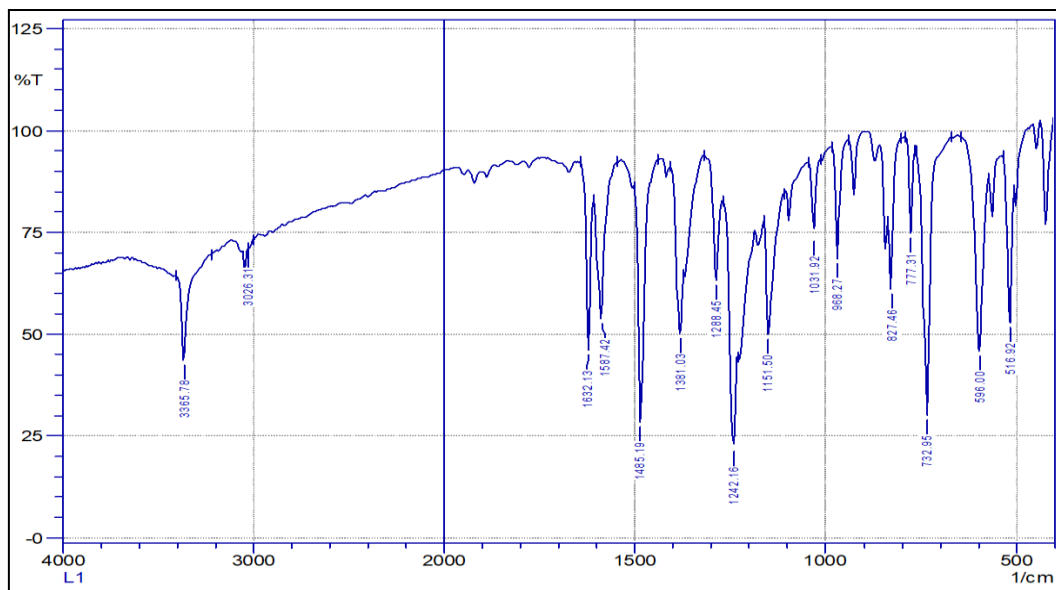


Figure 1 Infrared spectrum of the L

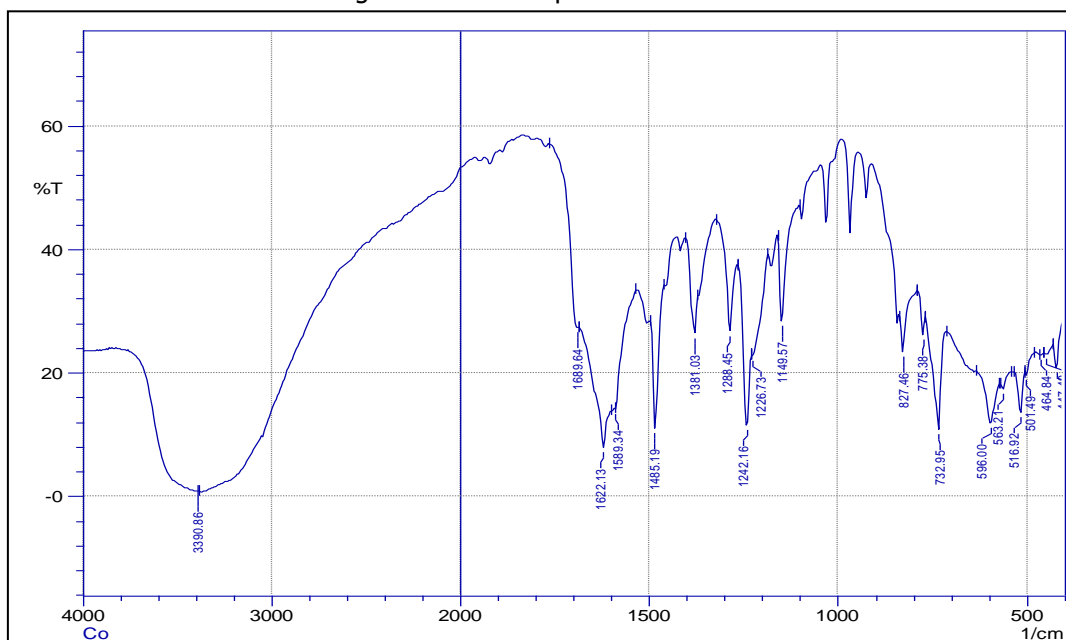


Figure 2 Infrared spectrum of the CuL

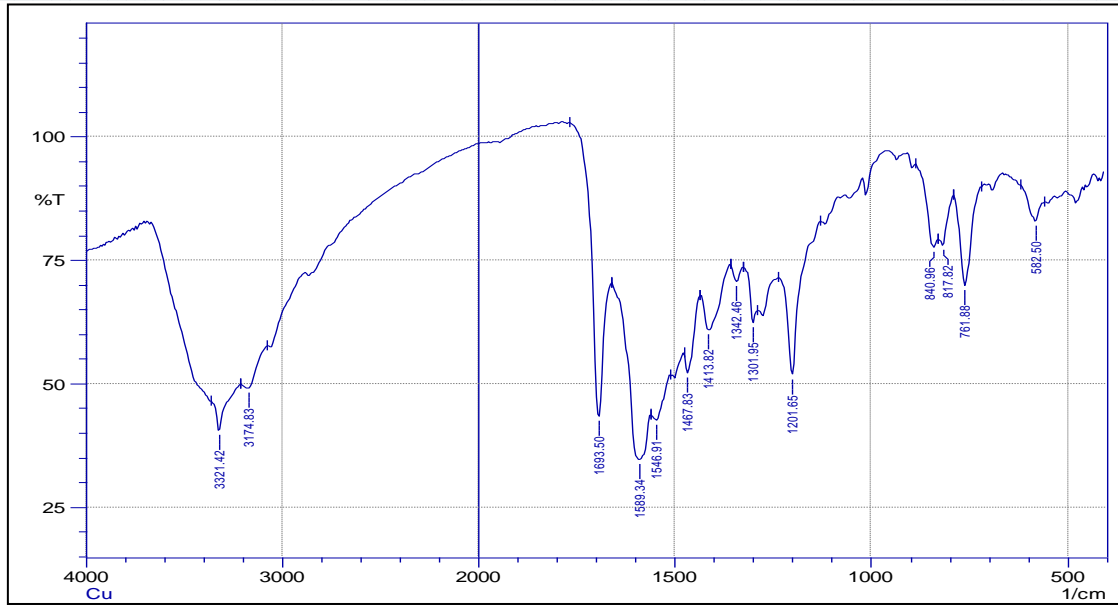


Figure 3 Infrared spectrum of the CuL

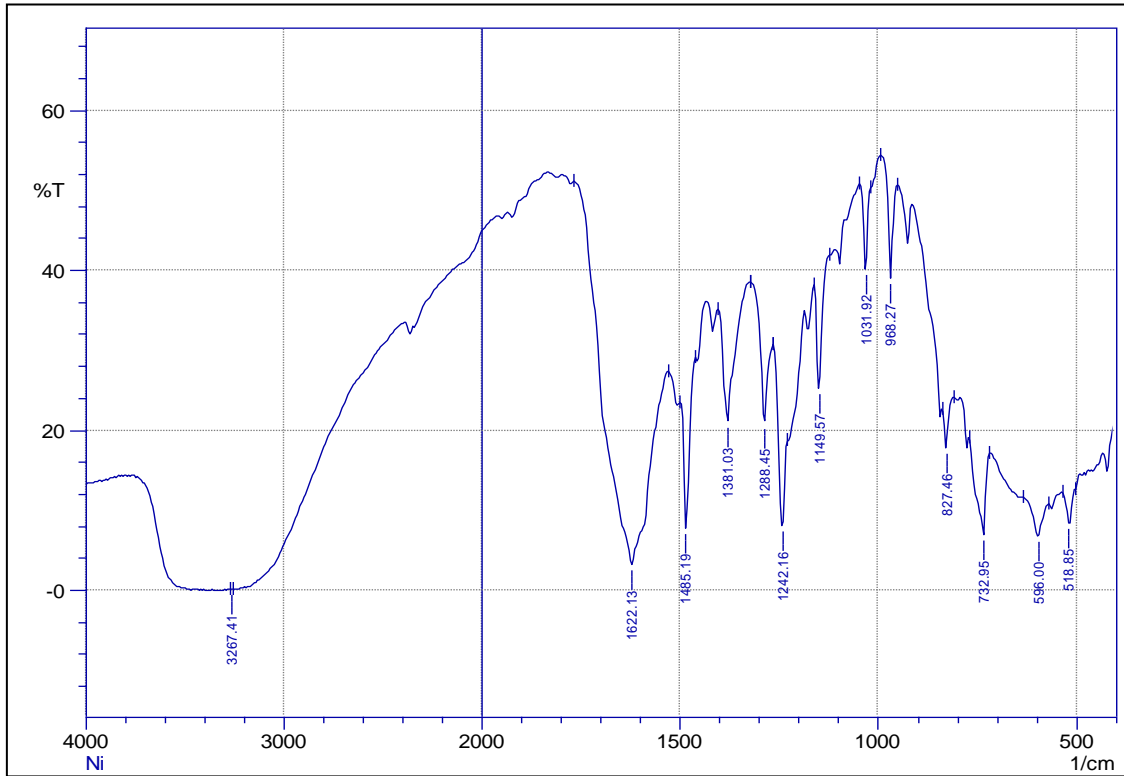


Figure 4 Infrared spectrum of the NiL

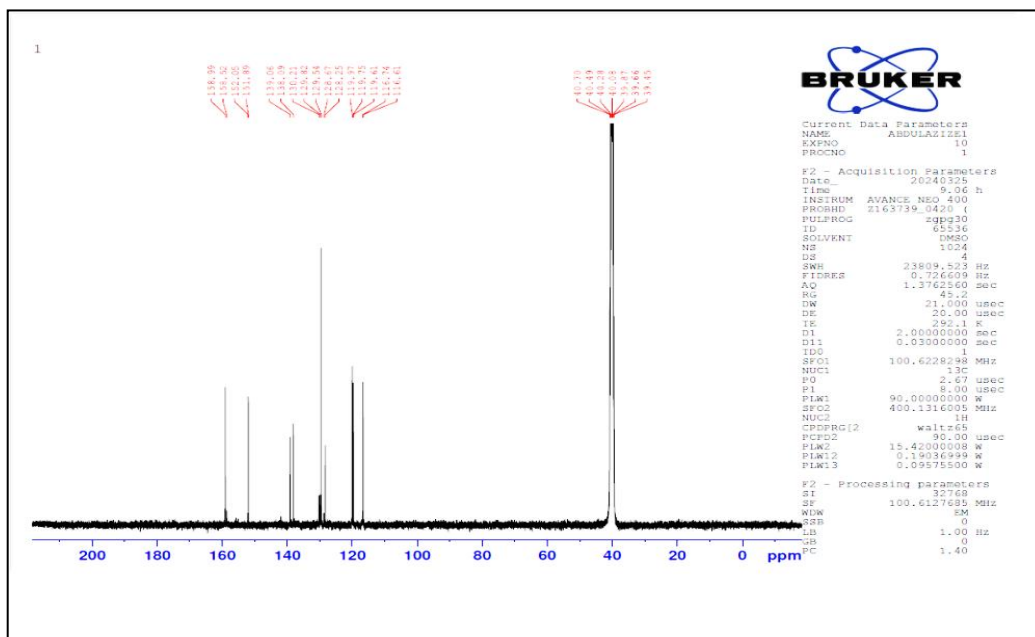


Figure 5: <sup>1</sup>Hnmr spectrum of the L

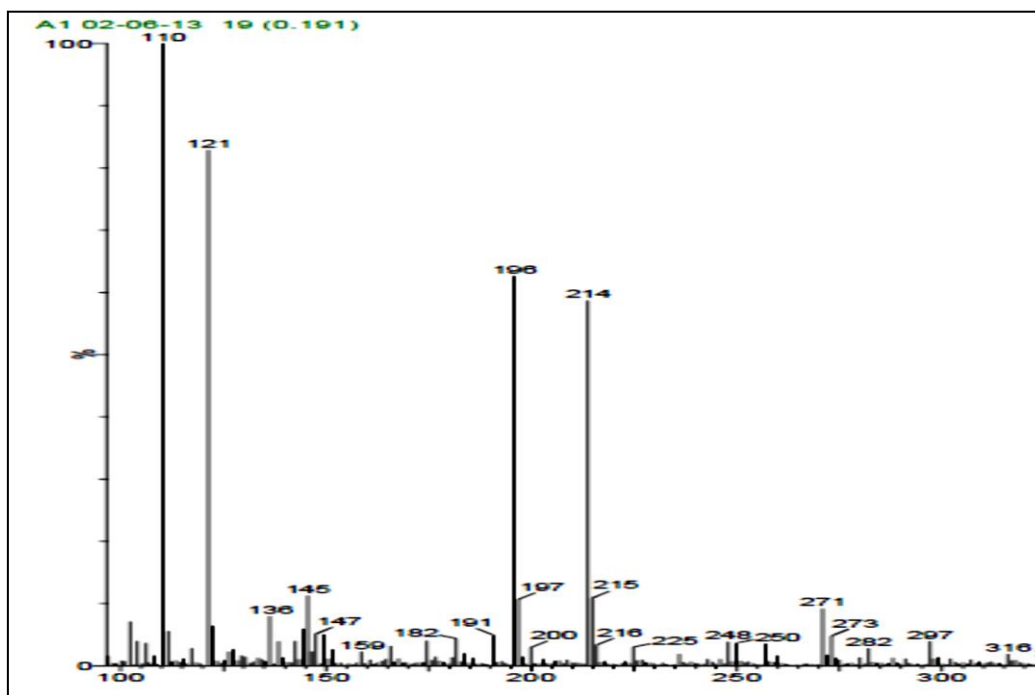


Figure 6: <sup>13</sup>Cnmr spectrum of the L

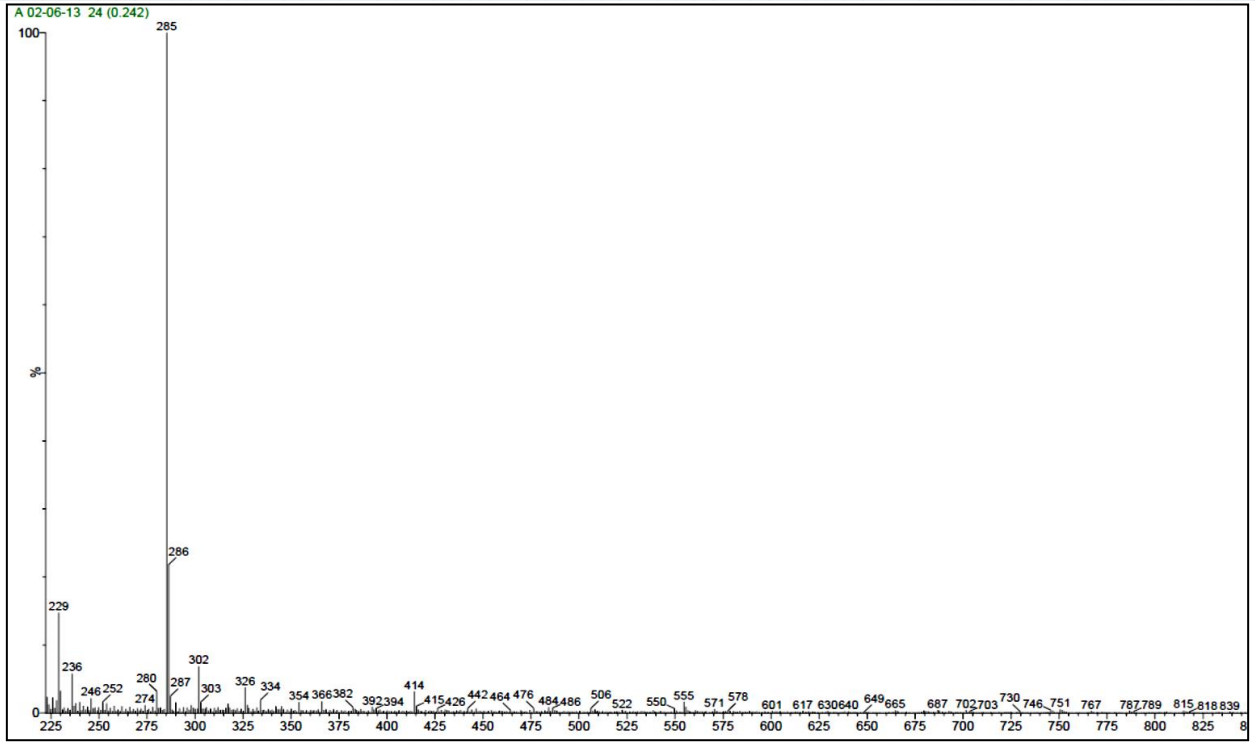


Figure7 mass spectra of the L.

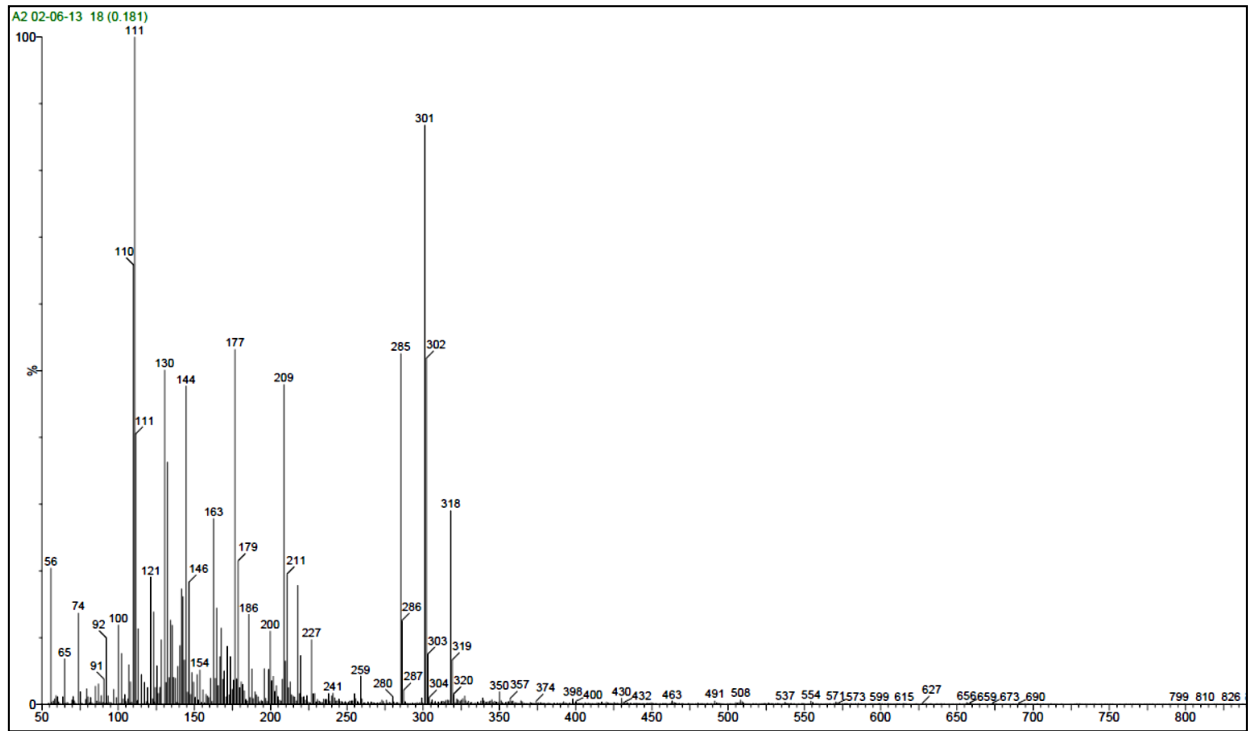


Figure 8 mass spectra of the CuL.

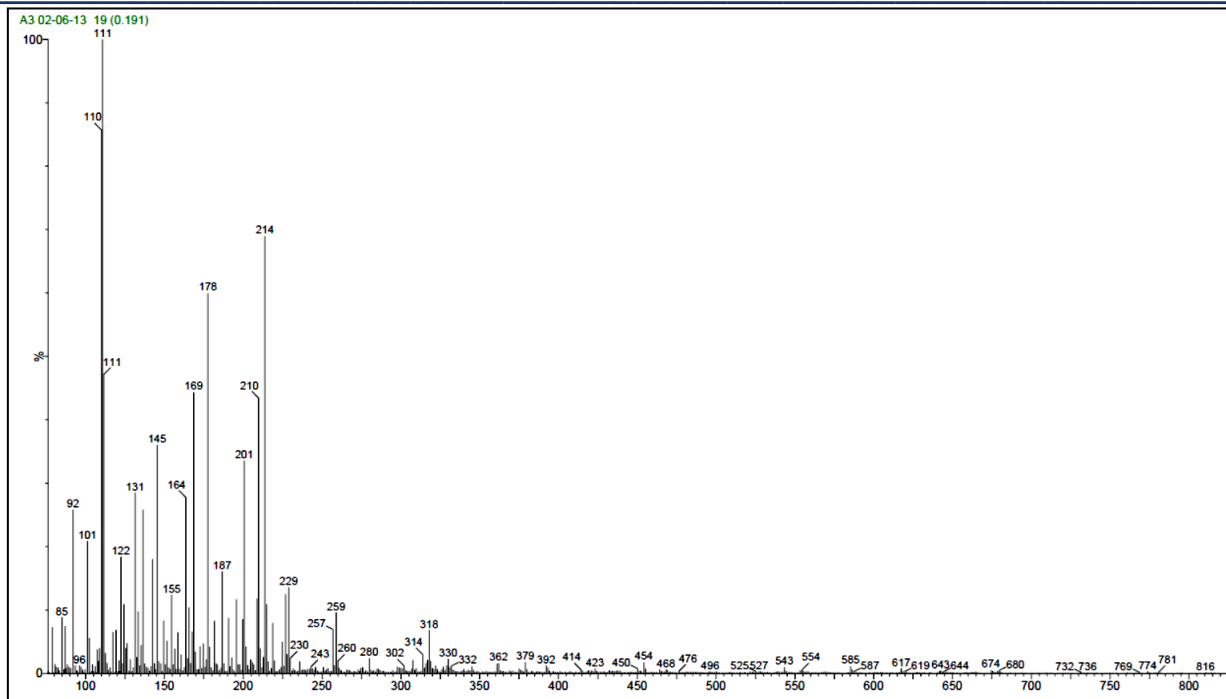


Figure 8 mass spectra of the CoL.

Table 1 Electronic Spectra for Ligand's and it's complexes

Compound	*( $\pi$ - $\pi$ ) phenyl Cycle (nm)	-C=N-( $\pi$ - $\pi$ ) (nm)	(d-d) (nm)
L	270	435	--
L Co	285	385	540
L Cu	290	380	380 555
L Ni	290	385	510 575

Table 3 Magnetic Susceptibility of complexes

Syml. Of complex	Formula of complex	Mass magnetic susceptibility $X_g \cdot 10^{-6}$	Molar magnetic susceptibility $X_m \cdot 10^{-6}$	Correc. factor $D \cdot 10^{-6}$	Atomic magnetic susceptibility $X_A \cdot 10^{-6}$	Effective magnetic moment $\mu_{eff}$ (B.M.)	Hybridization
<b>LCo</b>	$C_{40}H_{36}Co_2N_4O_8$	7.8012	3241.854	180.9	3049.984	2.845	$sp^3d^2$
<b>LCu</b>	$C_{40}H_{36}Cu_2N_4O_8$	4.110	1384.231	182.1	1569.774	1.782	$sp^3d^2$
<b>LNi</b>	$C_{40}H_{36}Ni_2N_4O_8$	5.587	2210.080	179.8-	2023.295	2.1	$sp^3d^2$

Sym	Molecular formula	Cell Constant A (cm)	Electrical Conductivity $Ohm^{-1}$	Molar Conductivity $Ohm^{-1} \cdot cm^2 \cdot mol^{-1}$
L-Co	$C_{40}H_{36}Co_2N_4O_8$	1.1	$19 \times 10^{-6}$	19
L-Cu	$C_{40}H_{36}Cu_2N_4O_8$	1.1	$20 \times 10^{-6}$	20
L-Ni	$C_{40}H_{36}Ni_2N_4O_8$	1.1	$17 \times 10^{-6}$	17

### 3. Thermal analysis

The thermal analysis of the  $C_{40}H_{36}Co_2N_4O_8$  cobalt complex shows that it proceeds in two distinct phases. In the first phase the curve at 101-219°C indicates loss of  $(C_{12}H_{20}O_6)$  (obs. = 7.394mg; 133.8%). The second phase indicates weight loss (obs. = 6.173mg 26.6%). In the temperature range of 226-560°C with the loss of  $C_{12}H_{11}N_2$  predicted.

The thermal analysis of the copper complex  $C_{40}H_{36}Cu_2N_4O_8$  is in three different phases. Under the same conditions. In the first stage, the curve at 134-219 °C indicates the loss of  $(C_4H_{17}O_4)$  (obs. = 3.55mg; 15.63%). The second phase indicates weight loss (obs. = 110.06mg 44.25%). In the temperature range of 225-367°C with predicted loss of  $C_8H_3NO_3$ ). Phase III indicates weight loss (obs. = 0.795mg3.5%). in the temperature range of 475-547°C with loss of  $C=H_{10}N_2O$  predicted.

The thermal analysis of the nickel complex  $C_{40}H_{36}Ni_2Ni_2N_4O=$  is also in three different stages. In the first stage, the final curve at 49.5-142°C indicates the loss of  $C_{10}H_{16}O_6N$  (obs. = 3.11mg; 30.30%). The second phase of the curve indicates weight loss (obs. = 12.36mg 23%). In the temperature range of 155-321°C with predicted loss of  $C_{10}H_6N_2O_2$ ). Phase III indicates weight loss (obs. = 2.42mg23.6%). In the temperature range of 405-557°C with predicted loss of  $C_{12}H_2NO_2$  (Alshawi et al., 2015; Jarallah & Hadi, 2012).

### 4. Bacterial efficacy

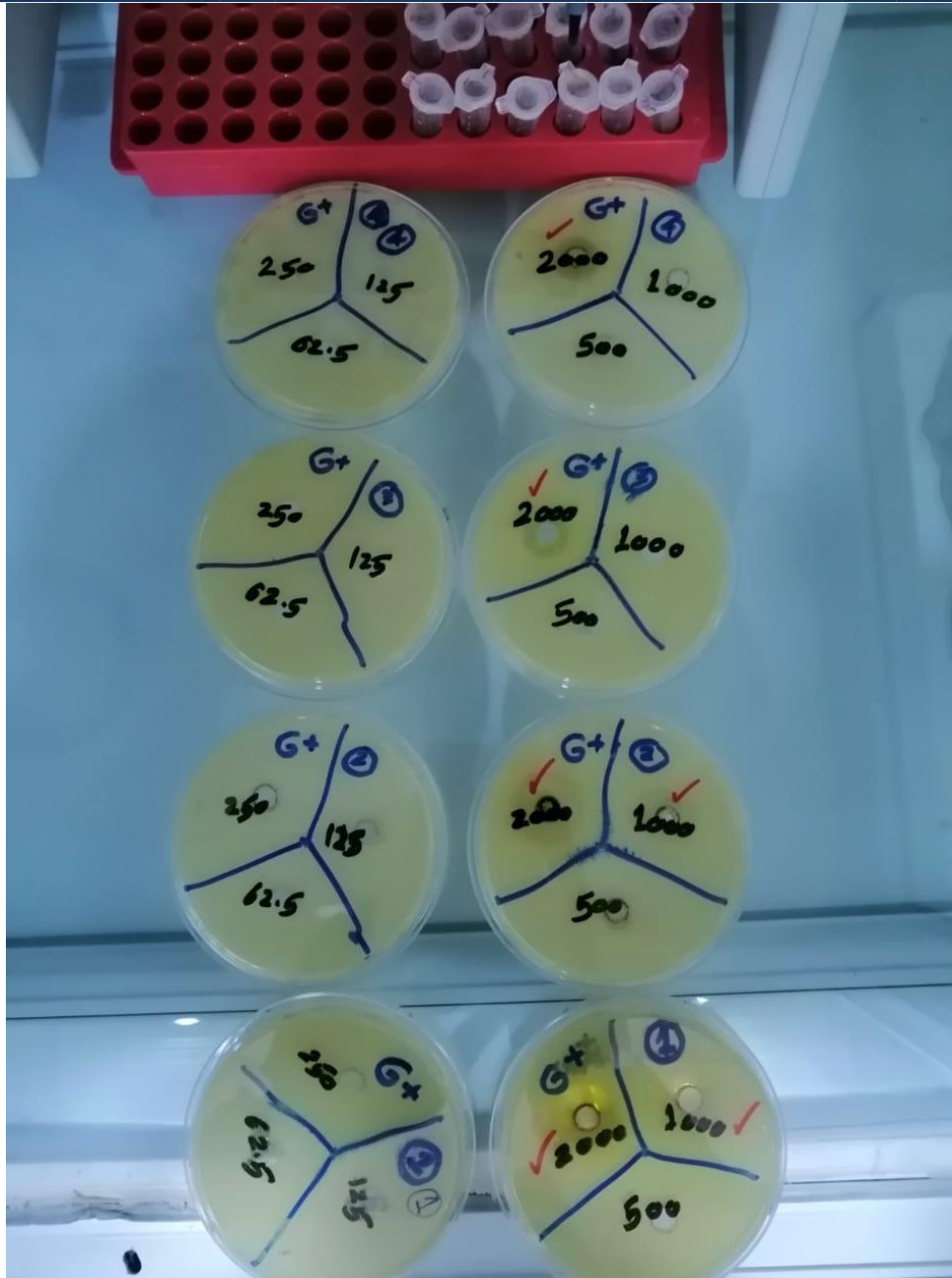
The bacteriological efficacy results of the prepared Schiff base ligand and its complexes presented in Table (28-3) indicate that the inhibition rates towards bacteria varied, and in general E.coli showed more resistance than S.aureus towards the compounds as shown in Figures (67-3) and (68-3). The cobalt complex gave good inhibition of S. aureus.

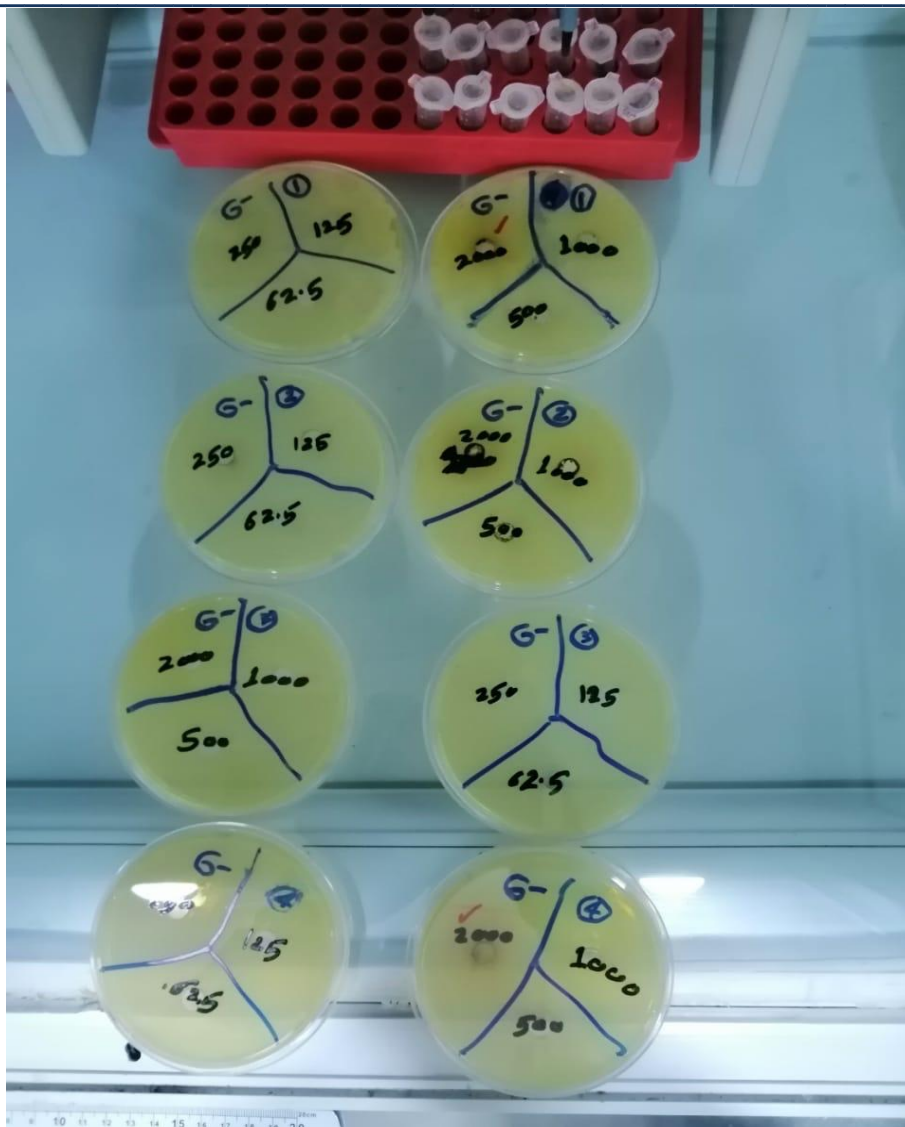
The increased inhibitory capacity of a compound depends on the ability of that compound to penetrate the bacterial membrane and enter the cell, as well as on the extent to which the metal atom affects normal cellular processes (208,207). Table (7-3) and Figures (18-3)-(19-3) show the zone of inhibition in centimetres for prepared Schiff bases and their complexes (Alshawi et al., 2020).

Table 4 Activity against Bateria of ligand and complexes

bacteria gram negative E.coli		
compound	concentration	inhibtion in cm
L=1	2000	1.4
LCo=2	2000	0
LCu=3	2000	0
LNi=4	2000	1.2
bacteria gram positive s. aurius		
L=1	1000	1
L=1	2000	2.8
LCo= 2	1000	1
LCo =2	2000	2.7
LCu=3	2000	1.5
LNi=4	2000	1.5







## 5. Conclusions

This ligand was characterised using FT-IR, UV-vis,  $^1\text{H-NMR}$ ,  $^{13}\text{C}$  and mass spectrometry and the prepared ligand was found to be donation as (NO). Complexes were prepared from the reaction of the prepared ligand with some transition elements  $\text{Cu}^{2+}$ ,  $\text{Co}^{2+}$ ,  $\text{Ni}^{2+}$  and were characterised by UV-vis, FT-IR, FT-IR, spectroscopy and conductivity. (IR), mass spectrum and molar conductivity which showed low values indicating that the complexes do not possess negative radicals outside the coordination sphere. The complexes were also subjected to thermogravimetric analysis (TGA) to see if these complexes contain water molecules coordinated to the central atom, and the magnetic properties of the prepared complexes were evaluated and the results showed that cobalt (II), copper(II) and nickel(II) complexes take an octahedral geometry and have paramagnetic properties.

Based on the different characterization methods described above, the structural formulae of the complexes were proposed. The Compounds under study gave good results against positive and negative bacteria, So we could do farther biological and theoretical studies to understanding the site effective of bacteria's protein.

## 6. REFERENCES

- Al-Zaidi, B. H., Hasson, M. M., & Ismail, A. H. (2019). New complexes of chelating Schiff base: Synthesis, spectral investigation, antimicrobial, and thermal behavior studies. *Journal of Applied Pharmaceutical Science*, 9(4), 45–57.
- Alshawi, J., Salih, Z., & Yassin, S. (2020). Synthesis, characterization and cytotoxic activity study of Cu (II), Co (II), Mn (II), Ni (II) and Cr (III) Metal Complexes with new guanidine Schiff base against the hepatocellular Carcinoma

- (HCAM) cancer cell. *Egyptian Journal of Chemistry*, 63(10), 2–3. <https://doi.org/10.21608/ejchem.2020.37893.2778>
- Alshawi, J., Yousif, M., Zangana, K. H., Vitorica Yrezabal, I. J., Winpenny, R., & Al-Jeboori, M. J. (2015). Crystal structure of diethyl 2,2'-[[(1E,1'E)-{[(1R,4R)-cyclo-hexane-1,4-di-yl]bis-(aza-nylyl-idene)}bis-(methanylyl-idene)]bis-(1H-pyrrole-2,1-di-yl)]di-acetate. *Acta Crystallographica. Section E, Crystallographic Communications*, 71(Pt 3), o165–6. <https://doi.org/10.1107/S2056989015002674>
- Annapure, S. R., Munde, A. S., & Rathod, S. D. (2016). Spectral, Thermal, X-Ray and Antimicrobial Studies of Newer Tetradentate N2O2 Schiff Base Complexes of First Transition Series. *Der Chemica Sinica*, 7(4), 47–54.
- Ashoor, L. S., Mohaisen, I. K., & Al-Shemary, R. K. R. (2020). A review on versatile applications of transition metal complexes incorporating schiff bases from amoxicillin and cephalexin. *EurAsian Journal of BioSciences*, 14(2), 7541–7550.
- Bejaoui, L., Rohlíček, J., Eigner, V., Ismail, A., El Bour, M., & Ben Hassen, R. (2019). Crystal Structure, Hirshfeld Surface Analysis and Biological Activities of trans-Dipyridinebis (3-Acetyl-2-Oxo-2H-Chromen-4-Olato) Cobalt (II). *Acta Chimica Slovenica*, 66(3).
- Du, H., Pang, X., Yu, H., Zhuang, X., Chen, X., Cui, D., Wang, X., & Jing, X. (2007). Polymerization of *rac*-Lactide Using Schiff Base Aluminum Catalysts: Structure, Activity, and Stereoselectivity. *Macromolecules*, 40(6), 1904–1913. <https://doi.org/10.1021/ma062194u>
- Fadhil, Z. S., Hassan, Q. M. A., Hussein, K. A., Sultan, H. A., Al Shawi, J. M. S., & Emshary, C. A. (2024). Studies of the nonlinear optical properties of a synthesized Schiff base ligand using visible cw laser beams. *Physica Scripta*, 99(6), 65525. <https://doi.org/10.1088/1402-4896/ad42e8>
- Garba, H. W., Abdullahi, M. S., Jamil, M. S. S., & Endot, N. A. (2021). Efficient catalytic reduction of 4-nitrophenol using copper (II) complexes with N, O-chelating schiff base ligands. *Molecules*, 26(19), 5876.
- Jarallah, H. M., & Hadi, J. S. (2012). Synthesis, characterization and thermal studies of 4-(2-hydroxy-3-methoxybenzylidene amino)-N-(pyridine-2-yl) Benzene Sulphonamide and their complexes. *Journal of Basrah Researches ((Sciences))*, 38(1).
- Kalaivani, S., Priya, N. P., & Arunachalam, S. (2012). Schiff bases: facile synthesis, spectral characterization and biocidal studies. *Int J App Bio Pharm Tech*, 3, 219–223.
- Lidskog, A., Li, Y., & Wärnmark, K. (2020). Asymmetric Ring-Opening of Epoxides Catalyzed by Metal–Salen Complexes. *Catalysts*, 10(6), 705. <https://doi.org/10.3390/catal10060705>
- Maleev, V. I., Chusov, D. A., Yashkina, L. V., Ikonnikov, N. S., & Il'in, M. M. (2014). Asymmetric ring opening of epoxides with cyanides catalysed by chiral binuclear titanium complexes. *Tetrahedron: Asymmetry*, 25(10–11), 838–843. <https://doi.org/10.1016/j.tetasy.2014.04.012>
- Reddy, A., Jyothi, S., Someshwar, P., & Swamy, S. J. (2016). New Pd (II) and Pt (II) Schiff Base Complexes for Catalytic Applications in CH Bond Activation and Oxygenation of Hydrocarbons. *Journal of Applicable Chemistry*, 5(5), 1146–1162.
- Savalia, R. V., Patel, A. P., Trivedi, P. T., Gohel, H. R., & Khetani, D. B. (2013). Rapid and economic synthesis of Schiff base of salicylaldehyde by microwave irradiation. *Research Journal of Chemical Sciences* ISSN, 2231, 606X.
- Taha, P. H., Al-Dabbagh, S. A., & Salh Esmael, B. M. (2022). Psychological Distress among Internet Addicted Undergraduates in Duhok-Iraq. *Arab Journal of Psychiatry*, 33(1).
- Taylor, J., Hafner, M., Yerushalmi, E., Smith, R., Bellasio, J., Vardavas, R., Bienkowska-Gibbs, T., & Rubin, J. (2014). Estimating the economic costs of antimicrobial resistance. *Model and Results (RAND Corporation, Cambridge, UK)*.
- Vishwa, P., Nagaraj, M., Palanivel, S., Annaiah, T., Prakash, S., Vinith Kumar, R., Rudregowda Sarojamma, V., & Kandaiah, S. (2024). Incorporation of Ruthenium Ions into Nanometer-Thick Films of Copper Sulfide by Anodization for Proton-Coupled Electron Transfer Reactions. *ACS Applied Nano Materials*, 7(4), 4453–4464.